Polymer 50 (2009) 3250–3258

Contents lists available at ScienceDirect

Polymer

journal homepage: www.elsevier.com/locate/polymer

Amplifying the molecular sieving capability of polyimide membranes via coupling of diamine networking and molecular architecture

Bee Ting Low [a], Youchang Xiao [a], Tai Shung Chung [a,b,*]

[a] Department of Chemical and Biomolecular Engineering, National University of Singapore, 10 Kent Ridge Crescent, Singapore 117602, Singapore
[b] Singapore–MIT Alliance, National University of Singapore, 10 Kent Ridge Crescent, Singapore 117602, Singapore

ARTICLE INFO

Article history:
Received 24 January 2009
Received in revised form
14 April 2009
Accepted 25 April 2009
Available online 6 May 2009

Keywords:
Molecular design
Diamine modification
Free volume and rigidity

ABSTRACT

The integration of molecular design with diamine modification generates synergistic effects for enhancing and fine tuning the molecular sieving potential of polyimide membranes. Polymer free volume and rigidity represent crucial conformational parameters that influence the effectiveness of diamine modification for elevating the H_2/CO_2 permselectivity of polyimide membranes. Experimental and molecular dynamics simulation results suggest that polyimides with higher intrinsic free volume and rigidity are ideal for diamine treatment, yielding greater increment in H_2/CO_2 selectivity. A series of copoly(4,4′-diphenyleneoxide/1,5-naphthalene-2,2′-bis(3,4-dicarboxylphenyl) hexafluoropropane diimide) (6FDA-ODA/NDA) membranes are modified with 1,3-diaminopropane (PDA). Polyimides with higher free volume intensify the methanol swelling effect which facilitates the transport and subsequent reaction of the diamine molecules. Gel content analyses of the PDA-modified films prove that the penetration depth of the diamine molecules and the extent of crosslinking are higher for polyimides with greater NDA content. 6FDA-NDA has the highest free volume and rigidity, thus exhibiting impressive improvement in ideal H_2/CO_2 selectivity from 1.8 to 120 after PDA modification. Conversely, 6FDA-ODA which is deficient in terms of free volume and rigidity, demonstrates a much lower increment in H_2/CO_2 selectivity from 2.5 to 8.2. The inherent heterogeneity of the PDA-modified polyimide films results in thickness-dependent gas permeability and selectivity. The potential of merging macromolecular tailoring with diamine networking to enhance the H_2/CO_2 separation performance of polyimide membranes is evident.

1. Introduction

The hypothetical hydrogen economy is envisioned as the optimal solution for global sustainability, in terms of controlling greenhouse gas emission and reducing worldwide dependence on oil [1,2]. Nevertheless, significant barriers to the extensive use of hydrogen as fuel are inevitably present. In midst of the wide array of challenges pertaining to the future success of the hydrogen economy, hydrogen purification and storage emerged as the overriding concerns [1]. Currently, large scale hydrogen generation is obtained via steam reforming of methane followed by the water–gas shift reaction [1–4]. The product stream leaving this unit operation contains carbon dioxide as the key contaminant. Hydrogen purification to eliminate CO_2 is therefore of paramount importance. Conventional separation processes (e.g. pressure swing adsorption and cryogenic distillation) for hydrogen enrichment are highly capital and energy intensive [1,2]. Conversely, membrane based separation is more energy efficient and environmentally friendly [1–6]. The future promises of the hydrogen economy have stimulated the interest of many researchers to develop high performance membranes for H_2/CO_2 separation.

Polymers are attractive materials for fabricating gas separation membranes because of their processability and affordable costs. Generally, glassy polymers are H_2-selective while rubbery polymers are CO_2-selective [3,4,7–11]. Each membrane type has its pros and cons, and the ultimate choice of the membrane is largely dependent on the operating conditions and applications. Glassy aromatic polyimides display superior physiochemical properties desirable for making gas separation membranes and there are numerous active studies on novel polyimides which are specifically engineered to enhance gas transport properties [12–25]. A comprehensive literature survey on engineered polyimides reported in the past two decades is conducted [24–41]. The H_2/CO_2 separation performances of the polyimide membranes are plotted against the Robeson trade-off line as depicted in Fig. 1 [42,43]. Recently, Robeson revisited the upper bounds for various gas pairs including H_2/CO_2 [43]. The minor shift and skew observed in the present H_2/CO_2 upper bound are attributed to the discovery of highly permeable polymers e.g. poly(trimethylsilylpropyne) [43].

* Corresponding author. Tel.: +65 68746645; fax: +65 67791936.
E-mail address: chencts@nus.edu.sg (T.S. Chung).

0032-3861/$ – see front matter © 2009 Elsevier Ltd. All rights reserved.
doi:10.1016/j.polymer.2009.04.059

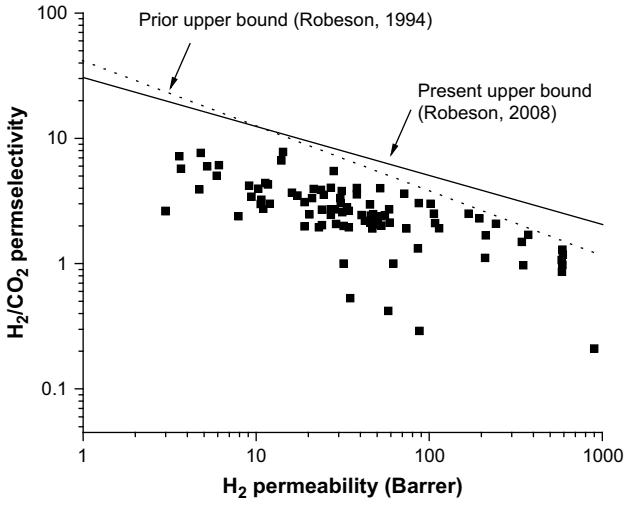

Fig. 1. Robeson plot of molecularly designed polyimide membranes.

Despite the continuous efforts by membrane scientists to explore novel polyimides via the permutations of different diamines and dianhydrides, the H_2/CO_2 separation performances of these materials remain nevertheless inferior. The H_2/CO_2 selectivity of polyimide membranes generally falls in the range of 0.2–7.8 [24–41]. Generally, the marginal increment in H_2/CO_2 selectivity obtained from the molecular design of polyimides does not compensate for the marked decline in H_2 permeability. For instance, Liu et al. investigated the gas transport properties of 4,4′-(hexafluoroisopropylidene) diphthalic anhydride (6FDA)-durene/sulfone-containing diamine (3,3′-DDS) copolyimides and found that increasing 3,3′-DDS content from 25 to 75 mol% improves H_2/CO_2 selectivity from 2.3 to 5.5 but a drastic drop in the corresponding H_2 permeability from 85 to 5 was observed [25]. Similar conclusions can be inferred from other related works, whereby the gain in H_2/CO_2 selectivity at the expense of H_2 permeability is simply not justifiable [24,28–30].

In a nutshell, the molecular architecture of polyimides is ineffective for H_2/CO_2 separation and polyimide membranes display intrinsic H_2/CO_2 permselectivity that are not attractive for commercial applications. Based on the solution-diffusion mechanism for gas transport across dense polymeric membranes, the gas pair (A/B) permselectivity is governed by the diffusivity (D_A/D_B) and solubility (S_A/S_B) selectivities. For the H_2/CO_2 pair, D_{H2}/D_{CO2} is generally greater than unity since H_2 has smaller molecular dimension. On the contrary, S_{H2}/S_{CO2} is smaller than one due to the higher critical temperature and condensability of CO_2. The physical properties of H_2 and CO_2 are listed in Table 1 [30]. Another factor that possibly contributes to the high CO_2 solubility in polyimide membranes is the favorable interactions between quadrupolar CO_2 molecules and the electrophilic imide groups that constitute the polymer. The undesirable coupling of these parameters results in poor intrinsic H_2/CO_2 permselectivity of numerous polyimide membranes.

Since molecular design of novel polymers fails to generate significant breakthroughs for high performance H_2-selective polymeric membranes, alternative approaches including chemical modification, polymer blending, carbonization and organic–inorganic hybrids have been investigated [3,44–51]. Among these options, the diamine modification of polyimide membranes has been demonstrated to effectively enhance the intrinsic H_2/CO_2 separation performance [3,44–51]. In a pioneering work by Chung et al., it was found that the modification of 6FDA-durene with aliphatic diamines notably enhances H_2/CO_2 selectivity [3]. For instance, the chemical modification of 6FDA-durene with 1,3-diaminopropane for 5 min brings about a 100 fold increment in H_2/CO_2 selectivity [3]. The applicability of this modification approach on polyimide membranes was verified in subsequent studies by Shao et al., Low et al. and Aberg et al [44–46]. The improvement in H_2/CO_2 permselectivity is attributed to the fact that the enhancement in D_{H2}/D_{CO2} (i.e. better size sieving effects) more than compensates for the decrease in S_{H2}/S_{CO2} (i.e. greater CO_2 sorption) after diamine modification [45]. It can be concluded from these works that the effectiveness of diamine modification in enhancing H_2/CO_2 selectivity greatly depends on the (1) electrophilicity and d-space of the polyimides, (2) nucleophilicity and molecular dimensions of the diamines and (3) modification duration [44–46].

A fundamental goal of our current research is to expand the H_2/CO_2 separation performance envelope defined by the permeability–permselectivity trade-off relationship. This study was undertaken to determine the feasibility of integrating molecular design with diamine modification for maximizing the molecular sieving potential of aromatic polyimide membranes. We envisage that this technique can be utilized to fine tune and optimize the enhancement in H_2/CO_2 separation factor achievable via diamine modification. In our previous work, copoly(4,4′-diphenyleneoxide/1,5-naphthalene-2,2′-bis(3,4-dicarboxylphenyl) hexafluoropropane diimide) (6FDA-ODA/NDA) films with equimolar composition of ODA to NDA (50:50) were modified with a series of aliphatic diamines with different spacer lengths [45]. It was determined that 1,3-diaminopropane is the most effective modification reagent for this polyimide [45]. The nucleophilicity and molecular dimensions of the diamines were identified as important parameters which influence the effectiveness of the modification [45]. This current work aims to elucidate and evaluate the effects of polyimide free volume and rigidity on the effectiveness of diamine modification. To better understand the role of polymer free volume and rigidity in the modification process, a series of 6FDA-ODA/NDA homo- and co-polyimides are employed for systematic investigation. Polyimides based on the same monomers are utilized to avoid complex interferences between the different functional groups and conformational properties on the gas separation performance. A critical assessment of the pristine and diamine-modified polyimide membranes for H_2/CO_2 separation via experimental and simulation approaches is presented.

Table 1
Physical properties of H_2 and CO_2.

	H_2	CO_2
Kinetic diameter, σ_k (Å)	2.98	3.30
Collision diameter, σ_c (Å)	2.92	4.00
Effective diameter, σ_{eff} (Å)	2.90	3.63
Critical temperature, T_c (K)	33.3	304.2
Molecule polarity	Non-polar	Quadrupolar

2. Experimental

2.1. Materials

The working polyimides were synthesized by the chemical imidization approach. The monomers 4,4′-(hexafluoroisopropylidene)diphthalic anhydride (6FDA), 4,4′-oxydianiline (ODA) and 1,5-naphthalenediamine (NDA) were sublimated under vacuum prior to use. 6FDA, ODA and NDA were purchased from Clariant (Germany), Sigma–Aldrich and Acros Organics, respectively. N-Methyl-2-pyrrolidone (NMP) from Merck was purified via vacuum distillation before use [45]. Different molar amounts of dianhydride and diamines were dissolved in NMP under nitrogen atmosphere to form a viscous solution of poly(amic acid). The total solid concentration was 20% by weight. 3-Picoline and acetic anhydride (molar

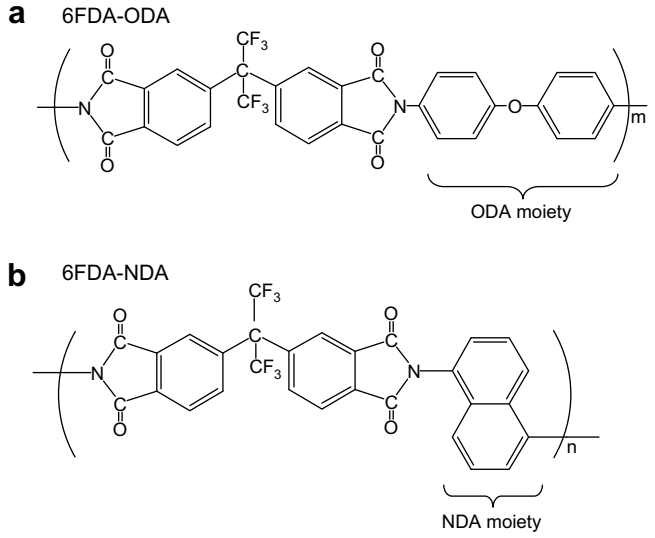

Fig. 2. Chemical structures of (a) 6FDA-ODA and (b) 6FDA-NDA homopolyimides.

ratio of 1:4) were added to form the polyimide. The polyimide solution was precipitated in methanol and dried under vacuum at 120 °C prior to use. The chemical structures of the homopolymers, 6FDA-NDA and 6FDA-ODA are shown in Fig. 2. A detailed description of the polymer synthesis can be obtained elsewhere [33,45]. Dimethylformamide (DMF) and methanol from Merck, and 1,3-diaminopropane (PDA) from Fluka were used as received.

2.2. Dense membrane fabrication and modification

A 2 (w/w)% of polymer solution was prepared by dissolving the respective polyimides in DMF [45]. The solution was stirred overnight and subsequently filtered using 1.0 μm PTFE membrane before ring casting onto a Si wafer plate at 55 °C to allow slow solvent evaporation [45]. After approximately one week, most of the solvent has evaporated, leaving behind the nascent film. Further heat treatment of the polyimide films was conducted under vacuum as follows: (1) hold at 60 °C for 24 h, (2) increase to 250 °C at 12 °C/20 min, (3) hold at 250 °C for 24 h and (4) natural cooling [45].

1.65 M of PDA in methanol solution was prepared for the chemical modification [45]. Each film was immersed in a fresh PDA/methanol solution for 90 min. The modified films were subsequently washed with methanol for 5 min to reduce the presence of residual unreacted diamines and dried at 70 °C under vacuum for 24 h for the removal of methanol [45].

2.3. Characterization

The changes in the chemical structure of the polymeric membranes before and after chemical modification were monitored by the attenuated total reflectance (ATR) mode using Bio-Rad FTIR FTS 135 over the range 650–2000 cm^{-1}. The number of scans for each sample was 32. XPS measurements were carried out by an AXIS HSi spectrometer (Kratos Analytical Ltd., England) using a monochromatized Al KR X-ray source (1486.6 eV photons) under vacuum environment. All core-level spectra were obtained at a photoelectron take-off angle of 90° with respect to the sample surface.

The gel contents of the PDA-modified films were determined by immersing the film in DMF for 5 days. The remaining insoluble portions of the membranes were dried under vacuum at 100 °C for 24 h to remove residual solvent before weighing. The gel content was calculated by equation (1)

$$\%\,\text{Gel content} = M_1/M_0 \times 100\% \quad (1)$$

where M_1 and M_0 are the mass of the insoluble fraction and the original mass of the PDA-modified films, respectively.

To investigate the degree of methanol swelling for the different polyimide films, the pristine films with thickness of 50 ± 5 μm were immersed in methanol for 90 min and dried in a vacuum oven at 70 °C for 24 h. The H_2 and CO_2 transport properties of the methanol-swelled films were determined. The relative increment in gas permeability indicates the extent of methanol swelling.

The changes in the intersegmental properties of the polymeric membranes were investigated using X-ray diffractor (XRD) Bruker, D8 series, GADDS (General Area Detector Diffraction System). Cu X-ray source of wavelength 1.54 Å was used. Average *d*-spacing was determined based on the Bragg's law as shown in equation (2)

$$n\lambda = 2d\sin\theta \quad (2)$$

where n is an integer (1,2,3, …), λ denotes the X-ray wavelength, d represents the intersegmental spacing between two polymer chains and θ indicates the diffraction angle.

The moduli of 6FDA-ODA and 6FDA-NDA films before and after PDA modification were measured by nanoindentation performed on a Hysitron Triboscope indenter system equipped with a Berkovich diamond tip. Loading and unloading rates of 100 μN/s were used. Five points were examined on each specimen and the mean moduli of the membranes were obtained.

2.4. Molecular simulations

Materials Studio 4.3 from Accelrys was used for molecular dynamics simulations. Repeat units of 6FDA-ODA and 6FDA-NDA were constructed using the "Build" function. 6FDA-ODA, 6FDA-NDA, and 6FDA-ODA/NDA copolymers were constructed using the as-built repeat units. For constructing the polymer, 10 repeat units were used with amino group as the initiator and terminator. Isotactic polymer configuration with random torsion and head-to-tail orientation were assumed for simulating the polymer chains. For the copolyimides, equal reactivity ratios and probability of the repeat units were assumed during the polymer construction. Energy minimization of the polyimide chains was performed prior to amorphous cell construction.

To simulate the dense polyimide membranes, the amorphous cell module was utilized for constructing a polymeric periodic cell based on compass forcefield calculations. The geometry of the configuration is allowed to be optimized following the construction of the amorphous cell. Ten polymer chains were used for construction. The amorphous cell was subjected to fine convergence with maximum iterations of 10,000 before proceeding with molecular dynamics simulation by the Discover module. An equilibrium stage temperature of 298 K and equilibrium time of 5.0 ps were used. Isothermal–isobaric (NPT) ensemble was used for the simulation. A total of 100,000 steps with a step time of 1.0 fs and a dynamics time of 100 ps were employed.

The free volume and occupied volume of each amorphous polyimide were calculated using the Connolly task [52]. Connolly radii that correspond to the kinetic diameters of H_2 and CO_2 molecules were used. The simulated fractional free volumes (FFV) of the polyimides are dependent on the chosen Connolly radius since these are used as the probe particles. The mean square displacements of the polyimide chains constituting the amorphous cells were determined using the Analysis function of the amorphous cell module. To investigate the effects of diamine modification on the polymer chain rigidity, 6FDA-ODA and 6FDA-NDA homopolyimides were chosen for representative studies. For each

polyimide, 2 chains with 10 repeat units were constructed and PDA linkages were built between consecutive imide rings on the respective polymer chains. The structures (with and without PDA crosslinking) were similarly subjected to minimization prior to molecular dynamics simulations. The mean square displacements of the polyimide chains with and without PDA crosslinking were compared.

2.5. Gas permeation tests

The pristine and PDA-modified dense membranes were tested for their H_2 and CO_2 permeation properties. Pure gas measurements were done using a variable-pressure constant-volume gas permeation cell. A detailed description of the permeation cell set-up and testing procedures can be obtained elsewhere [24]. The upstream pressure was 3.5 atm and the operating temperature was 35 °C. The rate of pressure increase (dp/dt) at steady state was used for the calculation of gas permeability according to equation (3)

$$P = \frac{273 \times 10^{10}}{760} \frac{Vl}{AT\left(p_2 \times 76/14.7\right)}\left(\frac{dp}{dt}\right) \quad (3)$$

where P is the gas permeability of a membrane in Barrer (1 Barrer $= 1 \times 10^{-10}$ cm^3 (STP)-cm/cm^2 s cmHg), V is the volume of the downstream chamber (cm^3), A refers to the effective membrane area (cm^2), l is the membrane thickness (cm), T is the operating temperature (K) and p_2 is the upstream pressure (psia).

The ideal permselectivity of a membrane for H_2 to CO_2, α was evaluated as follows.

$$\alpha = \frac{P_{H2}}{P_{CO2}} \quad (4)$$

where P_{H2} and P_{CO2} are the gas permeabilities for H_2 and CO_2, respectively.

3. Results and discussion

3.1. Characterization

The dense membranes before and after PDA modification were studied using ATR-FTIR. The characteristic peak representing C–F at 1242 cm^{-1} is used as the reference peak since the $C(CF_3)_2$ group is unaffected by the modification. With reference to Fig. 3(a), the pristine homo- and co-polyimides films exhibit a characteristic doublet at 1725 cm^{-1} and 1794 cm^{-1}, representative of the C═O group constituting the imide ring. The characteristic peak at 1362 cm^{-1} is attributed to the C–N stretch of the imide group while the peak at 1096 cm^{-1} is indicative of the transverse stretch of C–N–C in the imide group. The peak at 718 cm^{-1} is due to the out-of-plane bending of C–N–C in the imide group. The NDA moiety consists of naphthalene group which is clearly distinguishable from the ODA moiety. The weak peak at 1548 cm^{-1} and the doublet at 1605 cm^{-1} and 1629 cm^{-1} results from the C═C stretch of the naphthalene structure [53]. The strong peaks at 783 cm^{-1} and 1420 cm^{-1} are due to the disubstituted naphthalene structure and the out-of-plane vibrations of the three adjacent H atoms, respectively [53]. The various peaks in the region 1400–1000 cm^{-1} (including the strong peak at 1166 cm^{-1}) are representative of naphthalenes [53]. The characteristic peaks of ODA moiety includes 830 cm^{-1} and 1019 cm^{-1}, indicative of the out-of-plane deformation vibration of neighboring H atoms and 1,4-disubstituted benzenes, respectively [53].

Upon modifying the polymeric films with PDA, distinct peaks representative of the amide groups are clearly visible. Referring to Fig. 3(b), the characteristic peaks at 1648 cm^{-1} and 1540 cm^{-1} are attributed to C═O stretch and C–N stretch of the amide group, respectively. One observation is that the peaks representative of the amide groups are more prominent as the molar composition of NDA increases. The peaks representative of the imide groups are still present in 6FDA-ODA after PDA modification. This provides evidence that there is greater conversion from imide to amide

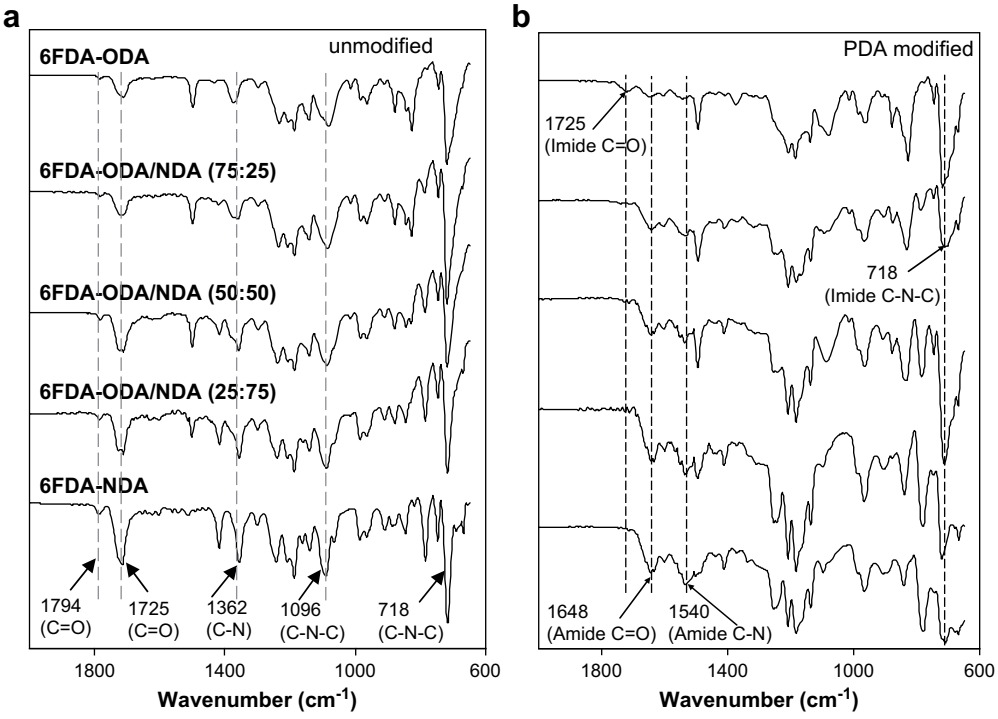

Fig. 3. FTIR spectra of (a) unmodified and (b) PDA-modified 6FDA-ODA/NDA films.

Table 2
Elemental composition of polyimide membrane surface before and after PDA modification determined by XPS.

Polymer	No modification			90 min PDA modification		
	N_{1s}	F_{1s}	N_{1s}/F_{1s}	N_{1s}	F_{1s}	N_{1s}/F_{1s}
6FDA-ODA	3.68	11.09	0.33	7.06	7.98	0.88
6FDA-ODA/NDA (75/25)	3.70	11.45	0.32	8.31	8.94	0.93
6FDA-ODA/NDA (50/50)	2.78	8.80	0.32	8.00	7.77	1.03
6FDA-ODA/NDA (25/75)	3.79	11.76	0.32	8.64	7.75	1.12
6FDA-NDA	4.42	12.78	0.35	9.20	7.91	1.16

groups for 6FDA-NDA homopolymer and copolymer with greater percentage of NDA moiety.

The elemental composition of the polyimide film surface was analyzed using XPS. The results are shown in Table 2. The N_{1s}/F_{1s} ratios of the synthesized polyimides are in the range 0.32–0.35. The theoretical N_{1s}/F_{1s} ratio for 6FDA-based polyimide is 0.33. After PDA modification, the N_{1s}/F_{1s} ratio increases with the molar composition of NDA which implies that a greater degree of amidation occurred for polyimides with higher NDA content. The higher nitrogen content after diamine modification is attributed to the following: (1) chemical grafting, (2) crosslinking and (3) presence of trace amounts of residual PDA molecules. This shows that the different diamine compositions of polyimide membranes affect the extent of modification.

The PDA-modified films were analyzed for the gel content and the results are presented in Table 3. The gel content of the PDA-modified film is an indication of the extent of crosslinking. The gel content increases as the molar composition of NDA in the polyimide increases. Thus, 6FDA-NDA exhibits the greatest degree of crosslinking.

An attempt to estimate the penetration depth of the PDA molecules from the film surface to the polymer bulk was performed. In our previous work, the estimation was achieved by means of the gel content analysis and a simplified resistance model [45]. Fig. 4 shows a schematic of the simplified resistance model. The resistance model is established based on the following assumptions: (1) homogenous modified layer, (2) negligible modification from the radial direction and (3) equal thickness of the top and bottom modified layers [45].

Here, the same approach was employed and the penetration depth of the PDA molecules is taken as the thickness of the top (or bottom) modified layer [45]. The estimated penetration depths are presented in Table 4. The penetration depth of the diamine molecules increases with the molar composition of NDA i.e. polyimide free volume.

To determine the inter-chain spacing of the polyimide films, XRD analysis was conducted and the spectra obtained for the unmodified and modified films are shown in Fig. 5 (a) and (b), respectively. The average *d*-space for 6FDA-NDA (5.73 Å) is the highest while the *d*-space for 6FDA-ODA (5.23 Å) is the smallest. Increasing the molar composition of NDA in the copolyimide results in larger chain-to-chain spacing since the introduction of the rigid NDA moiety disrupts the packing of the polymer chains. Hence, the free volume of the polymer increases with NDA content. For 6FDA-ODA polymer, there is a peak at $2\theta = 21.4^\circ$ which is indicative of the semi-crystalline nature of 6FDA-ODA [26]. No significant difference in the average *d*-space of the polyimide membranes before and after PDA modification was observed from XRD analysis.

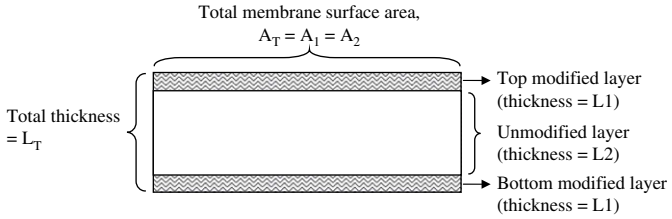

Fig. 4. Schematic of the simplified resistance model for the PDA-modified film [45].

The moduli of the 6FDA-ODA and 6FDA-NDA films before and after PDA modification were tested using nanoindentation and the results are summarized in Table 5. The modulus of 6FDA-NDA is approximately 50% greater than 6FDA-ODA. This outcome was within our expectation since the modulus of a material is related to its stiffness. The building blocks of 6FDA-NDA consist of highly rigid naphthalene structure while 6FDA-ODA comprises of flexible phenyl–O–phenyl linkages. For 6FDA-NDA, PDA modification for 90 min results in a 20% increment in modulus while for 6FDA-ODA, the changes in modulus after modification is negligible.

3.2. Molecular simulations

To mimic the packing of polyimide chains in dense membranes, amorphous cells packed with the respective polymers were simulated. The amorphous cell for 6FDA-NDA is depicted in Fig. 6. The Connolly algorithm was employed to determine the occupied and free volume within the amorphous cells [52]. Using these values, the fractional free volume (FFV) of the polyimide can be obtained from molecular simulations. The fractional free volume (FFV) of the 6FDA-based homo- and co-polyimides are summarized in Table 6. Referring to Table 6, increasing the NDA composition increases the FFV of the polymer. The packing density of the rigid 6FDA-NDA homopolyimide is the lowest, resulting in relatively more open and accessible cavities within the polymeric matrix. The reverse is true for the 6FDA-ODA polyimide. Two Connolly radii, each corresponding to the kinetic diameters of H_2 and CO_2 respectively, were used for estimating the polymer FFV. It has been highlighted in a work by Park and Paul that the polymer FFV is dependent on the nature of the gas penetrants and the universal applicability of the conventional group contribution approach for calculating the FFV is questioned [54]. Our simulated FFV results similarly suggest the dependence of the polymer free volume on the size of the gas penetrants.

To investigate the underlying motion of the molecules, the mean square displacements (MSD) of the polymeric chains within the amorphous cell were obtained from molecular dynamics simulations. The polymer chains in a solid matrix are in continuous motion and the MSD of a polymer is an important dynamic property that reflects the mobility of the polymer chains. By using the MSD instead of the displacement of the polymer chain, a scalar

Table 3
Gel content of PDA-modified polyimide films.

Polymer	Gel content (wt%)
6FDA-ODA	10 ± 2
6FDA-ODA/NDA (75:25)	14 ± 2
6FDA-ODA/NDA (50:50)	26 ± 4
6FDA-ODA/NDA (25:75)	43 ± 4
6FDA-NDA	55 ± 3

Table 4
Extent of PDA penetration during the modification of polyimide films.

Sample	Estimated penetration depth (μm)
6FDA-ODA	1.2 ± 0.4
6FDA-ODA/NDA (75:25)	3.5 ± 0.3
6FDA-ODA/NDA (50:50)	4.8 ± 0.8
6FDA-ODA/NDA (25:75)	11.4 ± 0.4
6FDA-NDA	14.7 ± 0.2

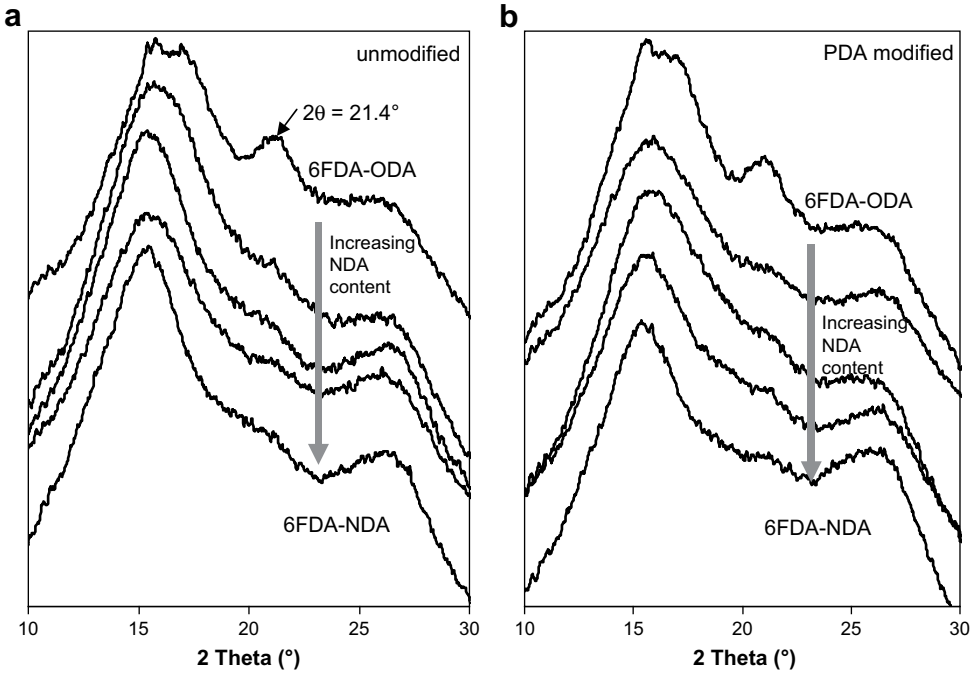

Fig. 5. WAXD spectra of (a) unmodified and (b) PDA-modified 6FDA-ODA/NDA films.

quantity is utilized instead of a vector, which better illustrates the overall mobility of the macromolecules. With reference to Fig. 7, 6FDA-ODA exhibits the greatest MSD while 6FDA-NDA shows the smallest MSD. Increasing the NDA composition increases the chain rigidity which in turn decreases the MSD of the polyimide chains.

3.3. Gas transport properties

The H_2 and CO_2 permeability coefficients of the 6FDA-ODA/NDA polyimides are shown in Table 7. The intrinsic gas permeability of this copolyimide series is coherent with the FFV of the polymers. A higher molar composition of NDA results in a greater FFV value and the corresponding gas permeability is higher. 6FDA-ODA exhibits the lowest gas permeability which is attributed both to its lower FFV and semi-crystalline structure. With reference to Table 7, it is obvious that the molecular design of this copolyimide series does not lead to significant changes in H_2/CO_2 selectivity. This conclusion is similar to those derived from previous works on polyimide designs [24–41]. Among these polyimides, 6FDA-NDA with the largest free volume results in the lowest intrinsic H_2/CO_2 selectivity while 6FDA-ODA with the lowest free volume results in marginally higher H_2/CO_2 selectivity.

Upon modifying the copolyimide membranes with PDA/methanol solution, significant changes in the H_2/CO_2 selectivity are observed. With reference to Table 7, 6FDA-NDA exhibits the greatest enhancement in H_2/CO_2 selectivity from an intrinsic value of 1.8 to an impressive separation factor of 120. The results obtained from our present work once again support the viability of the diamine modification for improving the H_2/CO_2 selectivity of polyimide membranes. It can be seen clearly from the results that increasing NDA composition leads to greater improvement in H_2/CO_2 selectivity when the same diamine modification conditions (i.e. 1.65 M PDA in methanol, modification duration of 90 min) were employed. 6FDA-ODA shows the least increment in H_2/CO_2 selectivity from 2.5 to 8.2. It is interesting to see that the ideal H_2/CO_2 selectivity trend is reversed after diamine modification. Polyimide with a higher intrinsic free volume leads to a greater decline in gas permeability after modification.

During the diamine modification process, the swelling of the polymer matrix by methanol occurs simultaneously with the chemical reactions taking place. This methanol swelling effect facilitates the transport of PDA molecules which in turn influences the extent of diamine modification. To investigate the different degrees of methanol swelling for the different polyimide films, the gas transport properties of the films after immersion in methanol are tested and presented in Table 8. The % increment in gas permeability after methanol swelling is higher for the polyimide with a greater NDA content. Methanol swelling is dependent on the intrinsic free volume and chain rigidity i.e. polymers with high free volume and chain flexibility are more easily swelled. From the results shown in Table 8, it is evident that the polymer free volume is the dominating factor for methanol swelling. The incorporation of NDA moiety in the polyimide leads to significant increment in free volume and amplifies the effects of methanol swelling. The presence of NDA moiety that increases the polymer chain rigidity fails to suppress the extent of methanol swelling. Polyimide with a higher free volume enhances methanol swelling which in turn facilitates the diffusion and reaction of diamine molecules within the polymeric matrix, giving rise to larger extent of modification. The greater degree of diamine-modified network with increasing NDA composition is proven by the higher N/F ratio from XPS analysis, the higher gel content and the prominent amide peaks shown by FTIR characterization. The space filling effect of the diamines within the polymer matrix decrease the available pathways for gas transport and enhance the diffusivity selectivity of H_2/CO_2 gas pair [45].

Table 5
Mechanical properties of pristine and PDA-modified homopolyimides.

Polymer	6FDA-ODA		6FDA-NDA	
	Pristine	PDA modified	Pristine	PDA modified
Modulus (GPa)	3.34 ± 0.16	3.53 ± 0.12	5.13 ± 0.25	6.19 ± 0.23

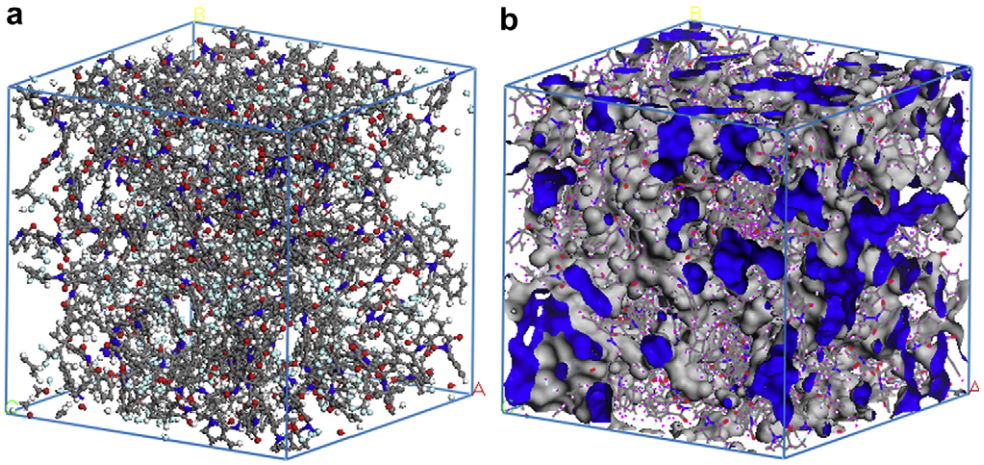

Fig. 6. (a) Simulated amorphous cell containing 6FDA-NDA homopolyimide chains and (b) occupied and free volume of the amorphous cell (grey: Van der Waals surface; blue: Connolly surface with probe radius of 1.49 Å).

Another possible factor that influences the effectiveness of diamine modification for enhancing the H_2/CO_2 selectivity of polyimide membranes is the polymer rigidity. Polymer rigidity is related to the chain stiffness and side group bulkiness. Generally, increasing the rigidity of the polymer chains leads to better H_2/CO_2 selectivity. The copolyimides employed in our work differ in the diamine moiety and the polymer rigidity is dependent on the chain stiffness rather than the side group bulkiness. The naphthalene structure in the NDA moiety gives rise to higher chain stiffness while the –O– connector linking the phenyl rings in ODA moiety results in greater flexibility. The MSD of the polyimide (Fig. 7) can be used to reflect the polymer rigidity i.e. rigid polymer exhibits lower MSD. Hence, based on the molecular simulations results, it can be inferred that the higher molar composition of NDA increases the rigidity of the polyimides.

When the polyimides are chemically modified with PDA, there are two intervening factors affecting the rigidity of the diamine-modified polymer. The breakage of the imide ring reduces the overall chain stiffness of the polymer. The attachment of the PDA moiety on the polyimide chain via the reaction of one NH_2 group with the imide ring is similar to the presence of a bulky side appendage on the polymer chain. This increases the rigidity of the modified polymer. To explore the effects of PDA modification on the polymer rigidity, molecular simulations were performed using 6FDA-NDA and 6FDA-ODA as the model polyimides. The mean square displacements of the polyimide chains before and after PDA crosslinking were determined. With reference to Fig. 8, the MSD of 6FDA-NDA chains decreases after PDA crosslinking. Hence, the rigidity of 6FDA-NDA increases after PDA crosslinking. The 20% increment in elastic modulus of 6FDA-NDA film after PDA modification (Table 5) similarly reflects the greater chain stiffness of the resultant polyimide matrix. This result is within our expectation since diamine crosslinking typically inhibits polymeric chain movements.

A surprisingly reverse trend in MSD was observed when 6FDA-ODA was subjected to PDA crosslinking. With reference to Fig. 9, PDA crosslinking decreases the MSD of 6FDA-ODA. This phenomenon can be adequately explained by taking a closer look at the chemical structures of the homopolyimides. For 6FDA-NDA, both the imide ring and naphthalene groups contribute to the polymer rigidity. After PDA modification, the rigid naphthalene structures maintain the backbone rigidity while the attachment of a PDA moiety constitutes a bulky side group to the polymer chain. Hence, the overall rigidity of 6FDA-NDA increases after PDA crosslinking. For 6FDA-ODA, the imide ring dominates the overall chain rigidity since the –O– linkage between two phenyl rings is relatively flexible. Therefore, the destruction of the imide ring upon PDA modification reduces the chain stiffness of 6FDA-ODA. The increase in polymer rigidity via the integration of PDA moiety does not compensate for the decrease in chain stiffness rooted from the cleavage of the imide rings. One point to highlight here is that despite the increase in the MSD of the 6FDA-ODA chains upon the incorporation of PDA, a slight improvement in H_2/CO_2 selectivity is nevertheless observed. The enhancement in H_2/CO_2 permselectivity after the PDA modification is attributed to an increase in chain rigidity, a decrease in free volume and a possible shift in the free volume distribution towards the smaller cavity sizes. The decrease in the free volume and the shift in free volume distribution are due to the space filling effects of the diamines [55,56]. Therefore, although PDA crosslinking of 6FDA-ODA leads to an increment in MSD (i.e. lowers chain rigidity) which should reduce H_2/CO_2 selectivity, the increment in the gas pair selectivity brought about by the reduction in free volume and the shift in the free volume distribution more than compensate for the

Table 6
Simulated FFV of copolyimides.

Properties	Molar ratio of ODA to NDA				
	100:0	75:25	50:50	25:75	0:100
FFV (H_2)[a]	0.1820	0.2069	0.2078	0.2169	0.2241
FFV (CO_2)[b]	0.1618	0.1870	0.1889	0.1977	0.2063

[a] Simulated FFV based on a Connolly radius of 1.49 Å.
[b] Simulated FFV based on a Connolly radius of 1.65 Å.

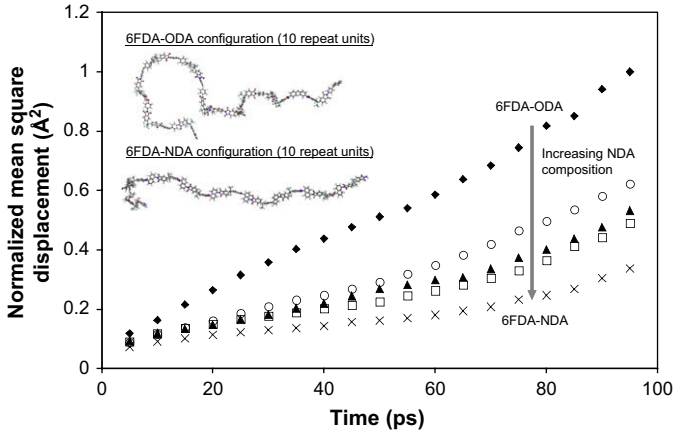

Fig. 7. Simulated mean square displacements of 6FDA-ODA/NDA copolyimides.

Table 7
H_2 and CO_2 transport properties of pristine and PDA-modified copolyimide films.

Polymer	No modification			PDA-modified for 90 min		
	Permeability (Barrer)		H_2/CO_2 selectivity	Permeability (Barrer)		H_2/CO_2 selectivity
	H_2	CO_2		H_2	CO_2	
6FDA-ODA	27	11	2.5	23	2.8	8.2
6FDA-ODA/NDA (75:25)	49	21	2.3	22	0.73	30
6FDA-ODA/NDA (50:50)	68	29	2.3	16	0.26	62
6FDA-ODA/NDA (25:75)	74	34	2.2	9.1	0.098	93
6FDA-NDA	78	43	1.8	12	0.10	120

Barrer $= 1 \times 10^{-10}$ cm^3 (STP)-cm/cm^2 s cmHg $= 7.5005 \times 10^{-18}$ m^2 s^{-1} Pa^{-1}.

decline. Hence, an overall marginal improvement in H_2/CO_2 selectivity was observed for 6FDA-ODA films. This suggests that the effectiveness of diamine modification is dependent on the intrinsic polymer rigidity. Diamine modification of polyimide with greater intrinsic rigidity leads to effective inhibition of chain movements which is favorable for improving H_2/CO_2 permselectivity.

Although the diamine modification of polyimide films is a good approach for enhancing the intrinsic H_2/CO_2 separation performance, it is important to note that the resultant films are not homogenous. This implies that the H_2/CO_2 transport properties are dependent on the film thickness. Therefore, we have chosen the 6FDA-ODA/NDA (50:50) polyimide for a representative study and films of different thicknesses were prepared and subjected to the same modification condition (i.e. 1.65 M PDA, 90 min). With reference to Table 9, as the film thickness increases, a considerable increase in gas permeability is observed while the corresponding gas pair selectivity decreases. This phenomenon can be adequately explained by the simplified resistance model (Fig. 4) for the PDA-modified films [45]. This model has been employed in Section 3.1 for estimating the penetration depth of the PDA molecules from the surface to the bulk of the polyimide films.

Based on the model, the H_2 and CO_2 permeabilities are represented by equations (5) and (6), respectively. The ideal H_2/CO_2 selectivity is given by equation (7).

$$\frac{L_{T,H2}}{P_{T,H2}A_T} = \left(\frac{2L_1}{P_1A_1} + \frac{L_2}{P_2A_2}\right)_{H2} \Rightarrow \frac{L_{T,H2}}{P_{T,H2}} = \left(\frac{2L_1}{P_1} + \frac{L_2}{P_2}\right)_{H2} \quad (5)$$

$$\frac{L_{T,CO2}}{P_{T,CO2}A_T} = \left(\frac{2L_1}{P_1A_1} + \frac{L_2}{P_2A_2}\right)_{CO2} \Rightarrow \frac{L_{T,CO2}}{P_{T,CO2}} = \left(\frac{2L_1}{P_1} + \frac{L_2}{P_2}\right)_{CO2} \quad (6)$$

$$\frac{P_{T,H2}}{P_{T,CO2}} = \frac{\left(\frac{2L_1}{P_1} + \frac{L_2}{P_2}\right)_{CO2}}{\left(\frac{2L_1}{P_1} + \frac{L_2}{P_2}\right)_{H2}} \quad (7)$$

P_T is the overall permeability and P_1 and P_2 refer to the permeabilities of the modified and unmodified layers. A refers to the membrane surface area as shown in Fig. 4.

Next, consider the system of membranes with different film thicknesses. Since the modification condition is the same, it is reasonable to assume that the thickness and permeability of the modified layer are similar i.e. P_1 and L_1 are constant. Another assumption is that the bulk of the membrane exhibits the same extent of methanol swelling regardless of the film thickness i.e. P_2 is constant. Hence, L_2 increases with increasing film thickness. Referring to equations (5) and (6), a larger L_2 leads to higher $P_{T,H2}$ and $P_{T,CO2}$. This accounts for the higher gas permeabilities as the film thickness increases from 30 μm to 100 μm. Similarly, the model can be used to explain the decline in H_2/CO_2 selectivity as the film thickness increases. A closer look at equation (7) reveals that $(L_1/P_1)_{CO2} >>> (L_1/P_1)H_2$. This implies that any increase in L_2 contributes more to the denominator term in equation (7). Therefore, a smaller $P_{T,H2}/P_{T,CO2}$ is obtained when the film thickness increases.

It is evident that both the polymer free volume and rigidity influence the effectiveness of the diamine modification which in turn determines that enhancement in H_2/CO_2 selectivity that can be achieved. One point to highlight here is that chain rigidity reflects the frustration in the packing of polymers which implies that the polymer free volume and rigidity are inter-dependent parameters. Based on the results obtained in this study, a polyimide with a higher free volume and rigidity (6FDA-NDA) would yield the greatest enhancement in H_2/CO_2 selectivity. This is attributed to the fact that polymer with a larger free volume allows for greater extent of diamine penetration and reaction while higher rigidity

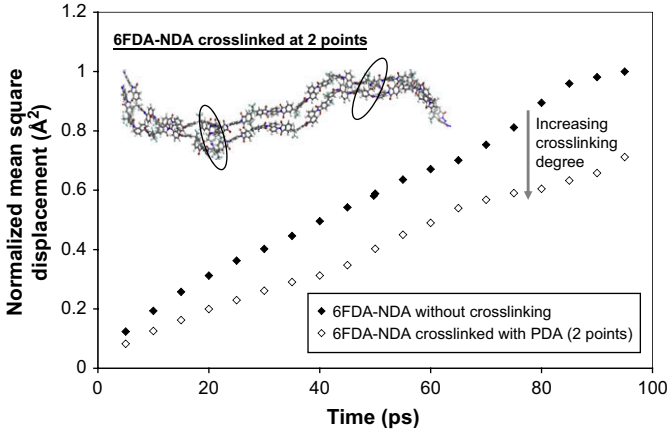

Fig. 8. Effect of PDA crosslinking on the mean square displacements of 6FDA-NDA polyimide chains.

Table 8
H_2 and CO_2 transport properties of methanol-swelled polyimide films.

Sample	H_2 permeability (Barrer)		% Increase	CO_2 permeability (Barrer)		% Increase
	Pristine	Methanol immersion		Pristine	Methanol immersion	
6FDA-ODA	27	34	26	11	14	27
6FDA-ODA/NDA (75:25)	49	64	31	21	31	48
6FDA-ODA/NDA (50:50)	68	98	44	29	51	76
6FDA-ODA/NDA (25:75)	74	152	105	34	95	179
6FDA-NDA	78	244	213	43	182	323

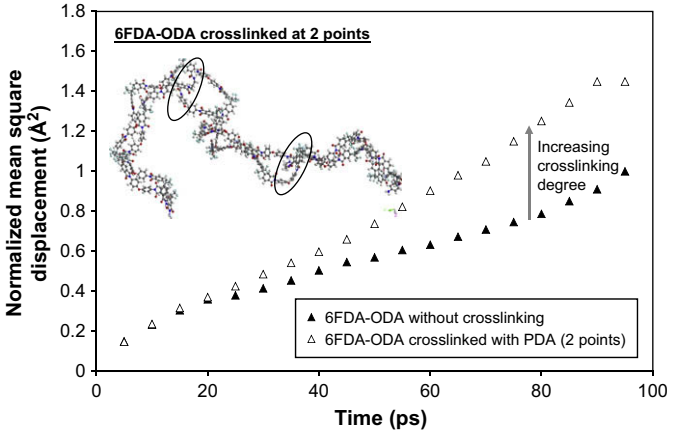

Fig. 9. Effect of PDA crosslinking on the mean square displacements of 6FDA-ODA polyimide chains.

Table 9
H_2 and CO_2 transport properties of PDA-modified 6FDA-ODA/NDA (50:50) films with different thickness.

Film thickness (μm)	H_2 permeability (Barrer)	CO_2 permeability (Barrer)	P_{H2}/P_{CO2}
30	9.1	0.14	65
50	16	0.26	62
70	27	0.49	55
100	33	0.83	40

enables the polymer to maintain or increase its chain stiffness. Both factors are favorable for improving the H_2/CO_2 selectivity of the polyimide membranes.

4. Conclusion

The coupling of polyimide molecular design and diamine modification represents an excellent approach for optimizing the enhancement in H_2/CO_2 permselectivity of polyimide membranes. We have identified two important parameters that influence the effectiveness of PDA modification in improving H_2/CO_2 selectivity i.e. polymer free volume and rigidity. Polymer free volume affects the degree of methanol swelling which in turn determines the extent of diamine penetration and reaction. Therefore, a polyimide with a higher free volume generates a denser diamine-modified network which is necessary for improving H_2/CO_2 selectivity. The H_2/CO_2 separation performance of the diamine-modified membranes is not merely dependent on the quantity but also the quality of the resultant chemical bridges. Polymer rigidity affects the ability of the polymer to maintain its chain stiffness upon the destruction of the imide rings during the diamine treatment. Hence, a polyimide with greater rigidity leads to a modified polymer network with restricted chain movements, thereby improving the H_2/CO_2 selectivity. Polyimides with high free volume and rigidity are ideal candidates for diamine modification and the enhancement in H_2/CO_2 selectivity that can be reaped is expected to supersede other polyimides.

Acknowledgements

The authors would like to thank the Singapore National Research Foundation (NRF) for the support on the Competitive Research Programme for the project entitled "Molecular Engineering of Membrane Materials: Research and Technology for Energy Development of Hydrogen, Natural Gas and Syngas" with grant number of R-279-000-261-281. Special thanks are dedicated to Dr. Abhijit Chatterjee from Accelrys for his assistance on molecular simulations. The valuable suggestions provided by Professor Donald Ross Paul, Dr. Lu Shao and Dr. Songlin Liu are greatly appreciated.

References

[1] Ockwig NW, Nenoff TN. Chem Rev 2007;107(10):4078–110.
[2] Shao L, Low BT, Chung TS, Greenberg AR. J Membr Sci 2008;327(1–2):18–31.
[3] Chung TS, Shao L, Tin PS. Macromol Rapid Commun 2006;27(13):998–1002.
[4] Lin H, Van Wagner E, Freeman BD, Toy LG, Gupta RP. Science 2006; 311(5761):639–42.
[5] Perry JD, Nagai K, Koros WJ. MRS Bull 2006;31(10):745–9.
[6] Baker R. Membr Technol 2001;2001(138):5–10.
[7] Qiu J, Zheng JM, Peinemann KV. Macromolecules 2007;40(9):3213–22.
[8] Lin H, Freeman BD. J Mol Struct 2005;739(1–3):57–74.
[9] Car A, Stropnik C, Yave W, Peinemann KV. J Membr Sci 2008;307(1):88–95.
[10] Merkel TC, Freeman BD, Spontak RJ, He Z, Pinnau I, Meakin P, et al. Science 2002;296(5567):519–22.
[11] Patel NP, Hunt MA, Lin-Gibson S, Bencherif S, Spontak RJ. J Membr Sci 2005;251(1–2):51–7.
[12] Chung TS, Chng ML, Pramoda KP, Xiao Y. Langmuir 2004;20(7):2966–9.
[13] Kim TH, Koros WJ, Husk GR, O'Brien KC. J Membr Sci 1988;37(1):45–62.
[14] Fub YJ, Hua CC, Qui HZ, Lee KR, Lai JY. Sep Purif Technol 2008;62(1):175–82.
[15] Wang YC, Huang SH, Hu CC, Li CL, Lee KR, Liaw DJ, et al. J Membr Sci 2005;248(1–2):15–25.
[16] Ayala D, Lozano AE, Abajo JD, Perez CG, Campa JG, Peinemann KV, et al. J Membr Sci 2003;215(1–2):61–73.
[17] Dai Y, Guiver MD, Robertson GP, Kang YS. Macromolecules 2005;38(23):9670–8.
[18] Guiver MD, Robertson GP, Dai Y, Bilodeau F, Kang YS, Lee KJ, et al. J Polym Sci Part A Polym Chem 2002;40(23):4193–204.
[19] Stern SA. J Membr Sci 1994;94(1):1–65.
[20] Stern SA, Mi Y, Yamamoto H, St. Clair AK. J Polym Sci Part B Polym Phys 1989;27(9):1887–909.
[21] Coleman MR, Koros WJ. Macromolecules 1999;32(9):3106–13.
[22] Cao C, Chung TS, Liu Y, Wang R, Pramoda KP. J Membr Sci 2003;216(1–2):257–68.
[23] Coleman MR, Koros WJ. J Polym Sci Part B Polym Phys 1994;32(11):1915–29.
[24] Lin WH, Vora RH, Chung TS. J Polym Sci Part B Polym Phys 2000;38(21):2703–13.
[25] Liu SL, Wang R, Chung TS, Chng ML, Liu Y, Vora RH. J Membr Sci 2002; 202(1–2):165–76.
[26] Coleman MR, Koros WJ. J Membr Sci 1990;50(3):285–97.
[27] Tanaka K, Kita H, Okamoto K, Nakamura A, Kusuki Y. J Membr Sci 1989; 47(1–2):203–15.
[28] Fang J, Kita H, Okamoto KI. J Membr Sci 2001;182(1–2):245–56.
[29] Al-Masri M, Kricheldorf HR, Fritsch D. Macromolecules 1999;32(23):7853–8.
[30] Liu SL, Wang R, Liu Y, Chng ML, Chung TS. Polymer 2001;42(21):8847–55.
[31] Staudt-Bickel C, Koros WJ. J Membr Sci 1999;155(1):145–54.
[32] Shishatskiy S, Nistor C, Popa M, Nunes SP, Peinemann KV. Adv Eng Mater 2006;8(5):390–1.
[33] Lin WH, Chung TS. J Membr Sci 2001;186(2):183–93.
[34] Xu JW, Chng ML, Chung TS, He CB, Wang R. Polymer 2003;44(16):4715–21.
[35] Yamamoto H, Mi Y, Stern SA, St. Clair AK. J Polym Sci Part B Polym Phys 1990;28(12):2291–304.
[36] Stern SA, Vaidyanathan R, Pratt JR. J Membr Sci 1990;49(1):1–14.
[37] Hao J, Tanaka K, Kita H, Okamoto KI. J Polym Sci Part A Polym Chem 1998;36(3):485–94.
[38] Kim KJ, Park SH, So WW, Ahn DJ, Moon SJ. J Membr Sci 2003;211(1):41–9.
[39] Tanaka K, Kita H, Okano M, Okamoto KI. Polymer 1992;33(3):585–92.
[40] Wang Z, Chen T, Xu J. Macromolecules 2000;33(15):5672–9.
[41] Xu ZK, Böhning M, Springer J, Glatz FP, Mülhaupt R. J Polym Sci Part B Polym Phys 1997;35(12):1855–68.
[42] Robeson LM, Burgoyne WF, Langsam M, Savoca AC, Tien CF. Polymer 1994; 35(23):4970–8.
[43] Robeson LM. J Membr Sci 2008;320(1–2):390–400.
[44] Shao L, Liu L, Cheng SX, Huang YD, Ma J. J Membr Sci 2008;312(1–2):174–85.
[45] Low BT, Xiao Y, Chung TS, Liu Y. Macromolecules 2008;41(4):1297–309.
[46] Aberg CM, Ozcam AE, Majikes JM, Seyam MA, Spontak RJ. Macromol Rapid Commun 2008;29(17):1461–6.
[47] Hosseini SS, Teoh MM, Chung TS. Polymer 2008;49(6):1594–603.
[48] Park HB, Jung CH, Lee YM, Hill AJ, Pas SJ, Mudie ST, et al. Science 2007;318(5848):254–8.
[49] Kim YK, Lee JM, Park HB, Lee YM. J Membr Sci 2004;235(1–2):139–46.
[50] Kim YK, Park HB, Lee YM. J Membr Sci 2005;255(1–2):265–73.
[51] Guiver MD, Thi NL, Robertson GP. U.S. Patent 2002/0062737 A1; 2002.
[52] User guide, visualizer tools section, calculating atom volume and surfaces, version 4.3. Accerlys Materials Studio; 2008.
[53] Socrates G. Infrared and Raman characteristic group frequencies: tables and charts. 3rd ed. New York: Wiley; 2000. p. 163–6.
[54] Park JY, Paul DR. J Membr Sci 1997;125(1):23–39.
[55] Xiao Y, Chung TS, Chng ML. Langmuir 2004;20(19):8230–8.
[56] Liu Y, Chung TS, Chng ML, Wang R. J Membr Sci 2003;214(1):83–92.